# On the Nature of Ti(IV)-Pillared Layered Metal Hydroxides Prepared from Green, Water-Soluble Ti-Peroxide

**Jing He, Huimin Shi, Xin Shu, and Minglin Li**
State Key Laboratory of Chemical Resource Engineering, Beijing University of Chemical Technology, Beijing 100029, China

*DOI 10.1002/aic.12029*
*Published online September 29, 2009 in Wiley InterScience (www.interscience.wiley.com).*

*Ti-peroxide pillared layered double hydroxides (LDHs) have been prepared for the first time using water-soluble Ti-peroxide as an intercalating precursor. It is novel and alluring that the whole preparation procedure does not involve any usage of organic or chlorine-containing hazards. Intercalated into the LDH interlayer region, Ti-peroxide is prevented partially from condensation in the solvent evaporation. The interlayer Ti—$O_2$ unit exists in triangular ($\eta^2$) structure with $C_{2v}$ symmetry in most cases, giving an interlayer gallery of 0.50–0.60 nm. But in the case of pH 4.0, monodentate ($\eta^1$) structure is also observed, giving an interlayer gallery of 0.70 nm. All the Ti-peroxide pillared LDHs prepared in this work show catalytic activity in the selective oxidation of thioether. The Ti-peroxide introduced into the interlayer regions of Mg/Al LDH with a particle size of around 50–120 nm exhibits better recyclability than Ti-peroxide gel, either in bulk or adsorbed on the exterior surface of LDH particles.* © 2009 American Institute of Chemical Engineers *AIChE J,* 56: 1352–1362, 2010

*Keywords: Ti-peroxide, intercalation, clean preparation, layered double hydroxides, heterogeneous catalyst*

## Introduction

As an environmentally friendly alternative to traditional stoichiometric processes, liquid-phase selective oxidation using clean and inexpensive $O_2$, $H_2O_2$, and $RO_2H$ as oxidants has been recognized to have enormous potential applications in organic synthesis. The liquid-phase oxidation technologies employing solid or immobilized catalysts[1–3] are particularly alluring because heterogeneous catalysts are easy to be recovered and facile to be recycled. Stimulated by the success of TS-1[4] in a variety of liquid-phase selective oxidations, a number of researches were performed on the synthesis and catalytic application of Ti(IV)-containing catalysts. Using organic orthotitanate as Ti(IV) precursors and surfactants or small organic compounds as structure-directing agents, Ti-containing microporous zeolites,[5,6] mesoporous materials,[6–8] or even titanium silicate analogous organic–inorganic hybrids[9] were prepared.

As one member of zeolite family, pillared layered catalysts could be formed readily in organic-free systems[10,11] through simple intercalation techniques. Layered materials could provide opportunities for developing new materials with a tailored nanodesign, tunable composition and properties, and controlled accessibility to the sites.[11–13] Ti(IV)-pillared montmorillonite materials were prepared[14–19] and applied as photocatalysts,[14] solid-acid catalysts,[15–16] and gas-phase oxidation catalysts.[20] The preparation methods in most cases involved the use of chloride-released $TiCl_4$.[14–18] Tungstate-intercalated,[21] Sn-exchanged,[22] V-pillared,[23] and Mo-loaded[21,24] layered double hydroxides (LDHs) were prepared for the liquid-phase oxidations of hydrocarbon compounds.

But the preparation and catalytic application of inorganic titanium-containing anions intercalated LDHs have not been reported previously.

Correspondence concerning this article should be addressed to J. He at jinghe@263.net.cn.

It is known that the clear aqueous solutions of Ti(IV) and hydrogen peroxide give yellowish to orange colors, characteristic of peroxo complexes, often referred to as peroxititanic acid. Although the formation mechanism of peroxititanic acid from titanium metal has not been completely understood, the reaction can be described as Eq. 1.[25]

$$\mathrm{Ti} + 3\mathrm{H_2O_2} \rightarrow \mathrm{Ti[(OH)_3O_2]^-} + \mathrm{H^+} + \mathrm{H_2O} \qquad (1)$$

Water-soluble titanium complexes Ti $[(OH)_3O_2]^-$ have proved to be promising reagents for the preparation of titanium-containing functional materials.[26–28] Hence, this work has employed water-soluble Ti-peroxide, a clean and environment-friendly Ti source, as a precursor to prepare Ti-peroxide pillared LDHs. The resultant Ti-peroxide encapsulated in the LDH interlayer domains have been applied as catalyst for the selective oxidation of thioethers in the liquid phase, using aqueous $H_2O_2$ as oxidant. The selective oxidations of thioethers, also called sulfoxidation, produce sulfoxides and sulfones that are widely used as drug, agrochemical, and synthetic intermediates.[29,30]

## Experimental

### *Chemicals*

Phenyl methyl sulfide (99.5%, Acros), hydrogen peroxide (30% in aqueous solution), and other reagents employed in this work are all of analytical purity and used as received without further purification. Deionized water, used in all of the precipitation, ion-exchange, and washing processes, were boiled to remove dissolved $CO_2$ (decarbonated) prior to use if not specified. Ti metal powder (99.9% of purity) is below the 200 mesh size.

### *Preparation*

The preparation of Ti-peroxide pillared LDHs and Ti-peroxide gel as control sample is illustrated in Figure 1.

*Water-Soluble Ti-Peroxide.* In a typical procedure, 0.50 g (0.01 mol) of titanium metal powder was dissolved in an ice-cooled solution of 30% $H_2O_2$ (100 mL, 0.92 mol), stirred for 1 h at 0°C and then for 9 h at 25°C, and filtered to yield a yellowish transparent solution. The pH of Ti $[(OH)_3O_2]^-$ solution was modulated using 13% $NH_3$ aqueous solution.

*M(II)/Al—$NO_3$ LDH-Coprecipitation.* M(II)/Al—$NO_3$ LDH-coprecipitation (M = Mg, Zn, or Ni) means that the LDH solids were synthesized by the coprecipitation approach. In a typical procedure, 1.8 M of alkaline solution (0.18 mol of NaOH in 100 mL of deionized water) was added dropwise into a mixture solution of 0.06 mol of $Mg(NO_3)_2$ and 0.03 mol of $Al(NO_3)_3$ dissolved in 100 mL of deionized water under thorough agitation in a $N_2$ flow, until the solution reached a pH of 10. The resultant slurry was crystallized at 100°C for 24 h and then centrifuged. The solid was washed extensively with deionized water and then dried in air at 80°C. Replacing $Mg(NO_3)_2$ with $Zn(NO_3)_2$ and $Ni(NO_3)_2$, Zn/Al—$NO_3$ LDH-coprecipitation and Ni/Al—$NO_3$ LDH-coprecipitation were prepared. The addition of alkaline solution ceased when the solution's pH reached 8 for the preparation of Zn/Al LDHs and 6 for Ni/Al LDHs. The crystallization temperatures for Zn/Al and Ni/Al LDHs are 100 and 80°C.

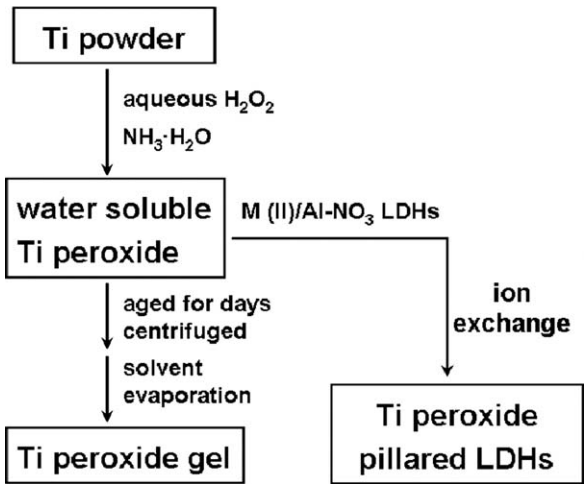


**Figure 1. Sketch illustration for the preparation of Ti-peroxide gel and Ti-peroxide pillared LDHs.**

*Mg/Al—$NO_3$ LDH-Homogeneous.* Mg/Al—$NO_3$ LDH-homogeneous was prepared by ion exchange of Mg/Al—$CO_3$ LDH-homogeneous with $NO_3^-$ in acidic solution. Mg/Al—$CO_3$ LDH was synthesized following a modified homogeneous approach as reported previously.[31] Typically, 0.02 mol of $Mg(NO_3)_2$ and 0.01 mol of $Al(NO_3)_3$ in 40 mL of deionized water, and 0.026 mol of hexamethylenetetramine in 40 mL of deionized water was loaded quickly under thorough agitation in a 100-mL Teflon autoclave. The resultant mixture solution was crystallized statically at 140°C for 24 h. Mg/Al—$CO_3$ LDH-homogeneous powdery product was collected by centrifugation. Mg/Al—$CO_3$ LDH-homogeneous (0.2 g) was suspended in 100 mL of acidic $NaNO_3$ aqueous solution (0.3 mol of $NaNO_3$ and 0.001 mol of $HNO_3$ in 100 mL of deionized water). The suspension was stirred at ambient temperature for 24 h under $N_2$ atmosphere. The resultant slurry was centrifuged. The solid was collected after being extensively washed with deionized water and dried at 80°C.

*Ti-Peroxide Pillared LDHs.* Ti-peroxide pillared LDHs were prepared through ion-exchange approach using M(II)/Al—$NO_3$ LDHs as hosts and water-soluble Ti-peroxide anion as an intercalating agent in an aqueous medium. Typically, 35 mL of 0.022 mol/L Ti $[(OH)_3O_2]^-$ aqueous solution (pH = 7.0 if not specially indicated, monitored with a pH meter) was mixed with LDHs suspended in 35 mL of deionized water. The Ti/Al molar ratio in the mixture suspension was 1.34 if not specially indicated. The resultant suspension was stirred at ambient temperature for 24 h under $N_2$ atmosphere and then centrifuged. The solid was washed with deionized water and vacuumed at ambient temperature for 6 h.

*Ti-Peroxide Gel.* The yellowish-transparent solution prepared earlier was precipitated at ambient temperature for 5 days. The yellow precipitate was centrifuged, dried at ambient atmosphere, and the resultant solid was ground for use.

### *Characterization*

Powder X-ray diffraction (XRD) data were collected on a Shimadzu XRD-6000 powder diffractometer using Cu K$\alpha$ ($\lambda$ = 0.1542 nm) radiation (40 kV and 30 mA) between 3

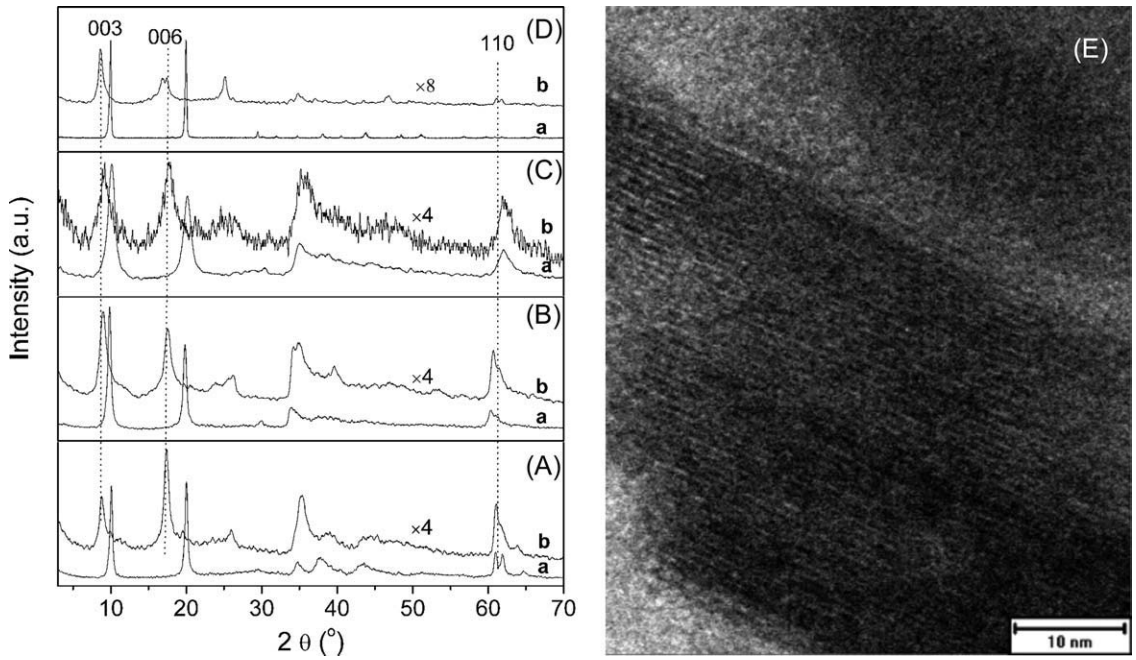


**Figure 2. XRD patterns of (A) Mg/Al—LDH-coprecipitation, (B) Zn/Al-LDH- coprecipitation, (C) Ni/Al-LDH-coprecipitation, (D) Mg/Al-LDH- homogeneous.**

(a) $NO_3$-LDHs and (b) Ti-peroxide pillared LDHs. (E) HRTEM of Ti-peroxide pillared LDH-coprecipitation.

and 70°, with a step size of 0.05° and a scanning rate of 5° $min^{-1}$. The in situ temperature-programmed XRD patterns were obtained on a PANalytical X'Pert PRO MPD diffractometer using Cu K$\alpha$ ($\lambda = 0.1542$ nm) radiation (40 kV and 40 mA) with a step size of 0.03°. The FT-IR spectra were recorded on a Bruker Vector 22 spectrometer at a resolution of 4 $cm^{-1}$, and the samples were being pressed into disks with KBr. FT-Raman spectra were recorded on a Nicolet Nexus 670 spectrometer at a resolution of 4 $cm^{-1}$. The contents of Mg, Al, Zn, Ni, and Ti were determined using ICP emission spectroscopy by dissolving the Ti-free samples in dilute $HNO_3$ and Ti-containing samples in the mixture solution (1:1, v/v) of $HNO_3$ and 30% $H_2O_2$. C, H, and N analysis was carried out on an Elementar Co. Vario El elemental analyzer. Scanning electron micrographs (SEMs) were taken on a HITACHI S-4700 SEM. The samples were ultrasonically dispersed in ethanol prior to SEM measurements. Transmission electron micrographs (TEMs) were taken on a JEOL-2010 TEM operating at 200 kV. Dark-field TEM micrographs were taken on a JEOL-2011 transmission electron microscope operating at 200 kV. The sample for TEM characterization was prepared by dipping carbon-coated copper TEM grids with a dilute ethanol suspension of the sample powder. TG-DTA-MS analysis was carried out on a Pyris Diamond/Thermaster TM spectrograph with a temperature-programmed rate of 10°C/min and a $N_2$ flow of 200 mL/min. The UV–vis diffuse reflectance spectra were collected on a Hitachi U-3010 spectrophotometer with a slit of 1 nm.

### *Catalytic tests*

Typically, the catalytic sulfoxidation was performed as follows. Catalyst (22.4 mg) was suspended in 10 mL of acetonitrile, with 1.0 mmol (117 $\mu$L) of thioether added. The reaction was started by the addition of 2.2 mmol of $H_2O_2$ (0.24 mL of 30% aqueous solution). The reaction mixture was continuously stirred at 40°C and sampled at intervals. The sampled liquor was added with 0.03 g of $Na_2SO_3$ to terminate the reaction and then filtered using a 0.20-$\mu$m microfilter. The supernatant was subject to GC-MS analysis on a Shimadzu GC-MS2010 with a DB-5 capillary column.

## Results and Discussion

### *Intercalation of Ti-peroxide in LDHs*

Mg/Al—$NO_3$ LDH-coprecipitation is first employed in this work for Ti-peroxide intercalation through ion exchange in aqueous solution using water-soluble Ti $[(OH)_3O_2]^-$ as intercalating agent. The XRD pattern of the resultant solid is shown in Figure 2A. The reflections can be indexed as a hexagonal unit cell with R-3m rhombohedral symmetry, which is generally observed for LDHs-type materials. The Ti-peroxide intercalation shifts (003) and (006) reflections from $2\theta = 10°$ and 20° to $2\theta = 8.7°$ and 17.4°, respectively. The basal spacing is expanded from 0.88 nm, the $d_{003}$ characteristic of $M(II)_2Al—NO_3$ LDHs, to 1.00 nm. An inversion in the relative intensity of (006) to (003) reflections is observed for the Ti-peroxide pillared Mg/Al LDH-coprecipitation. This inversion phenomenon has also been observed previously by Prévot et al.[32] and Beaudot et al.[33] for the LDHs intercalated with heavy-metal containing anions, and attributed to the increase of the electron density in the interlayer midplane.[33] So the intensity inversion of (006) relative to (003) diffraction in our case can be justified as a result of an ordered arrangement of Ti-peroxide species in the interlayer regions. Using $Zn_2Al—NO_3$ LDH-coprecipitation

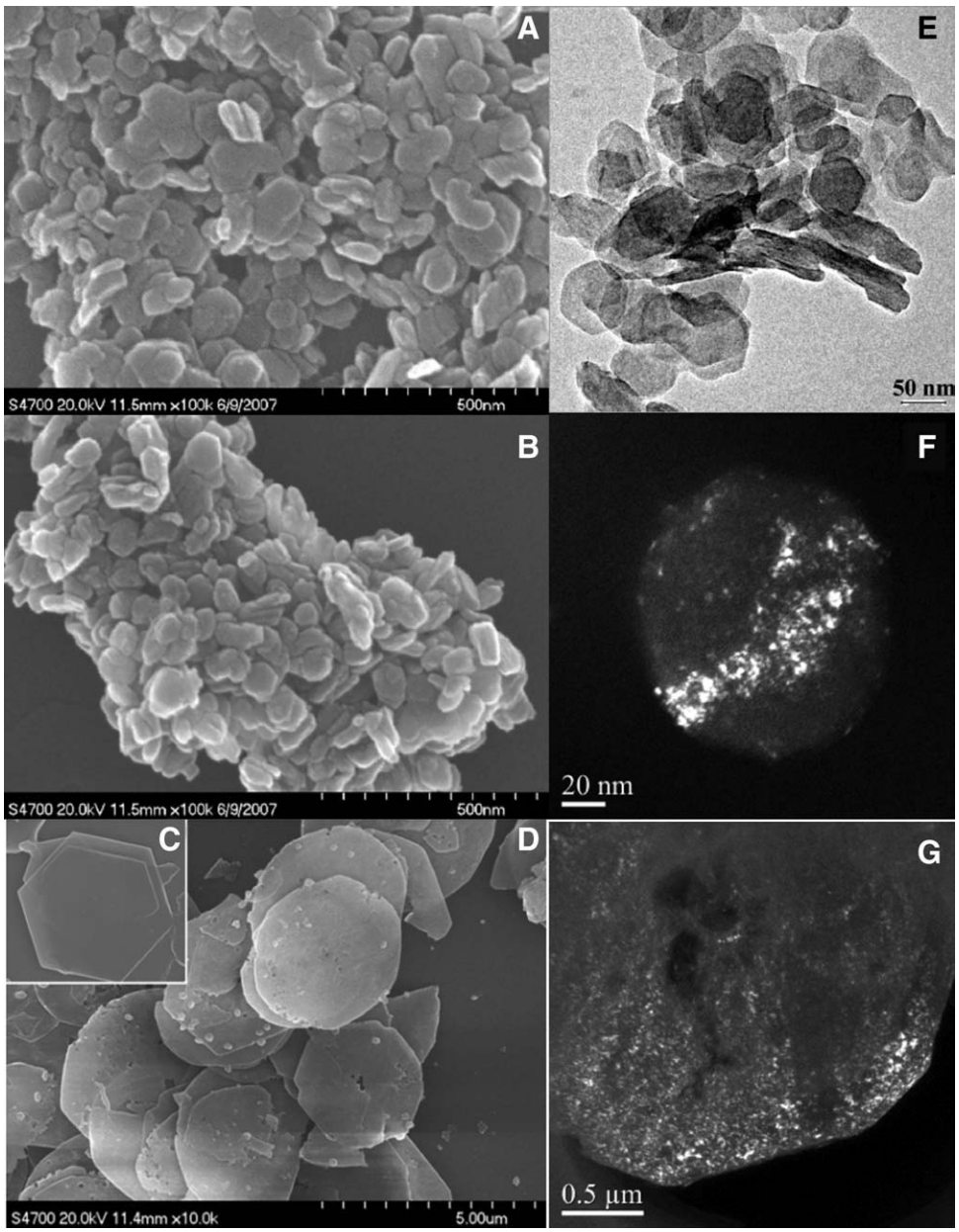


**Figure 3. SEM (A–D) and TEM (E–G) micrographs of Mg/Al—$NO_3$ LDH-coprecipitation (A), Ti-peroxide pillared LDH-coprecipitation (B, E, and F), Mg/Al—$NO_3$ LDH-homogeneous (C), and Ti-peroxide pillared LDH-homogeneous (D and G).**

The images (F) and (G) were taken in dark field.

(Figure 2B) and $Ni_2Al—NO_3$ LDH-coprecipitation (Figure 2C) as hosts, the XRD patterns typical of Ti-peroxide pillared LDH structures can be observed as well. The basal spacing is enlarged from 0.88 to 0.98 nm for Zn/Al LDHs and 0.97 nm for Ni/Al LDHs. The (006) reflections become more intensive than (003) because of the Ti-peroxide intercalation for Ni/Al LDH, similar to the one observed for Mg/Al LDH-coprecipitation. Subtracting the LDH layer thickness (0.48 nm) from the observed basal spacing, the interlayer gallery height is calculated to be 0.52, 0.50, and 0.49 nm for Ti-peroxide pillared Mg/Al, Zn/Al, and Ni/Al LDH-coprecipitaion. Well consistent with XRD measurements, an interlayer gallery of around 0.50 nm is estimated from the HRTEM image of Ti-peroxide pillared Mg/Al LDH-coprecipitaion (Figure 2E).

Generally, the homogeneous precipitation method produces LDHs with better crystallization and larger crystal size than the coprecipitation method.[10] Mg/Al—$NO_3$ LDH-homogeneous is thus prepared and subsequently ion-exchanged with water-soluble Ti-peroxide. The Mg/Al—$NO_3$ LDH-homogeneous displays intensive and symmetric XRD reflections typical of well-crystallized layered structure (Figure 2D). The Ti-peroxide intercalation expands the basal spacing of Mg/Al LDH-homogeneous from 0.88 to 1.08 nm (Figure

**Table 1. Chemical Composition of Ti-Peroxide Pillared LDHs**

| Ti-Peroxide Pillared LDHs | Chemical Composition (wt %) (found/cal) | | | | | Formula |
|---|---|---|---|---|---|---|
| | M(II) | Al | Ti | C | H | |
| Mg/Al-coprecipitation | 16.01/16.26 | 8.78/9.01 | 9.55/9.25 | 1.95/1.94 | 3.19/3.69 | $Mg_{0.67}Al_{0.33}(OH)_2[Ti(OH)_3O_2]^-_{0.16}$ $[HCO_3]^-_{0.15}[CO_3]^{2-}_{0.01}\cdot 0.51H_2O$ |
| Zn/Al-coprecipitation | 30.18/30.35 | 9.50/9.51 | 5.23/5.11 | 1.32/1.28 | 3.31/3.53 | $Zn_{0.57}Al_{0.43}(OH)_2$ $[Ti(OH)_3O_2]^-_{0.13}$ $[CO_3]^{2-}_{0.13}\cdot 0.81H_2O$ |
| Ni/Al-coprecipitation | 20.62/20.68 | 7.56/7.56 | 6.04/6.11 | 1.92/1.91 | 3.12/4.45 | $Ni_{0.56}Al_{0.44}(OH)_2$ $[Ti(OH)_3O_2]^-_{0.20}$ $[HCO_3]^-_{0.25}\cdot 2.07H_2O$ |
| Mg/Al- homogeneous | 17.18/16.96 | 10.31/10.28 | 4.45/4.18 | 1.81/2.09 | 4.14/4.03 | $Mg_{0.65}Al_{0.35}(OH)_2[Ti(OH)_3O_2]^-_{0.08}$ $[CO_3]^{2-}_{0.11}[HCO_3]^{2-}_{0.05}\cdot 0.71H_2O$ |

2D), giving an interlayer gallery height of 0.60 nm, which is similar to the one observed for Ti-peroxide pillared LDH-coprecipitation.

The planar plate-like particles of Mg/Al—$NO_3$ LDH-homogeneous are sized in 1–3 $\mu$m and Mg/Al—$NO_3$ LDH-coprecipitation in 50–120 nm, as estimated in SEM images (Figure 3). The Ti-peroxide intercalation causes no visible change in the plate-like morphology and particle size. The Ti-peroxide pillared LDHs still show typical hexagonal shape in the same size scale as their precursors. The Ti atoms, viewed by dark-field TEM micrographs (Figures 3F, G), are distributed throughout the interlayer regions for both nanosized Mg/Al LDH-coprecipitation and microsized Mg/Al LDH-homogeneous. The Ti distribution in nanosized LDHs is observed more densely, which might be associated with its higher Ti content. So, the determination of chemical composition is carried out.

The chemical compositions of Ti-peroxide pillared LDHs, determined by combining elemental analysis with ICP technique, are shown in Table 1. As can be seen in Table 1, the Ti content in the nanosized Mg/Al LDH-coprecipitation nearly doubles that in the microsized Mg/Al LDH-homogeneous. In each case, a nonnegligible amount of carbon element is detected. But as displayed in the XRD patterns, only one single Ti-peroxide intercalation phase has been resolved in each case (Figures 2A–D). The carbon element should thus be originated from the carbonate or dicarbonate as coexisting interlayer anions balancing the layer charges. It is worthy of note that, whether or not the (006) to (003) intensity inversion has been observed in the XRD patterns, it is well consistent with the Ti content in each sample. For the Ti-peroxide pillared Mg/Al LDH-coprecipitation and Ni/Al LDH-coprecipitation, in which the Ti species compensates more than 45% of the layer charges, an inversion or at least the enhancement of (006) reflection has been observed. For the Ti-peroxide pillared Zn/Al LDH-coprecipitation and Mg/Al LDH-homogeneous, however, in which the Ti species balances less than 30% of the layer charges, no intensity inversion of (003) and (006) reflections has taken place.

It is found in our work that Ti $[(OH)_3O_2]^-$ anion is energetic enough to exchange the interlayer $NO_3$- if the experiments have been well performed. As shown in Figure 4A, Ti-peroxide pillared LDH is produced as the main phase when the molar ratio of Ti $[(OH)_3O_2]^-$ to the Al in LDH layer (Ti/Al molar ratio) is as low as 1.00. But the competitive intercalation of $CO_3^{2-}$ anion is not absolutely excluded in this case even though the intercalation is performed under $N_2$ atmosphere. When the Ti/Al molar ratio is equal to 1.34 or higher, only Ti-peroxide pillared phase is observed. A Ti/Al molar ratio of less than 1.00 is not preferred because in that case $NO_3^-$ anions are not exchanged completely by Ti $[(OH)_3O_2]^-$, with the XRD reflections representing Mg/Al—$CO_3$, Mg/Al—$NO_3$, and Ti-peroxide pillared LDHs observed simultaneously. Taking account of the pH sensitivity[34] of Ti-peroxide species, pH has been varied to carry out the intercalation. It was reported that Ti peroxides were charged negatively at a pH higher than 3.[34] The Ti-peroxide intercalation has thus been carried out at pH = 4–9 in this work. From the XRD patterns shown in Figure 4B, it can be seen that the ion-exchange performed at pH 6 or 7 produces well-ordered Ti-peroxide pillared LDHs. The observation is logical because Ti$[(OH)_3O_2]^-$ is the absolutely predominating Ti species at a pH of $\sim$7.[34] Only weak and broad XRD reflections arising from Ti-peroxide pillared LDHs are observed at pH = 9, which should be closely related with the accelerated condensation of Ti-peroxo species at high pH. It is interesting that, under pH 4, in addition to the reflections of $NO_3$-LDHs at $d_{003}$ = 0.88 nm and the Ti-peroxide pillared LDHs usually observed at $d_{003}$ = 1.01 nm, there appears another reflection at $d_{003}$ = 1.18 nm. The new intercalation phase gives an interlayer height of 0.70 nm. We propose that the second Ti-peroxide pillared LDH structure results from the intercalation of another coexisting water-soluble Ti-peroxo species, which is to be discussed later. It has to be noted that the Ti-peroxo species at pH 4 is less competent for ion exchange, resulting in the incomplete disappearance of Mg/Al—$NO_3$ LDH as precursor.

### *Interlayer Ti-peroxo species*

Figure 5 illustrates the FT-IR and Raman spectra of Ti-peroxide encapsulated in the interlayer regions of LDHs. For comparison, the spectra for the bulk Ti-peroxide gel are also displayed. For the bulk Ti-peroxide gel, the broad IR bands (Figure 5A) associated with O—O vibrations, and symmetric and asymmetric vibrations of Ti—$O_2$ are centered at 832, 611, and 553 $cm^{-1}$. When intercalated into Mg/Al-LDHs, the Ti-peroxide shows broad IR absorptions around 865, 780, and 669 $cm^{-1}$. The band at 553 $cm^{-1}$ is overlapped with M—OH vibrations of LDH layers at 556 $cm^{-1}$. A shoulder band at 612 $cm^{-1}$ is observed for the Ti-peroxide in the interlayer region of Zn/Al or Ni/Al-LDHs. The corresponding frequencies for $\nu_s$ (O—O), $\nu_s$ (Ti—$O_2$), and $\nu_{as}$ (Ti—$O_2$) in Ti-peroxo complex crystals were ever observed around 876, 606, and 525 $cm^{-1}$,[35] or at 865 $cm^{-1}$, [26] 690, and 630 $cm^{-1}$,[36] approximately consistent with our observations. The absorption at 780 $cm^{-1}$ arises from the Ti—O

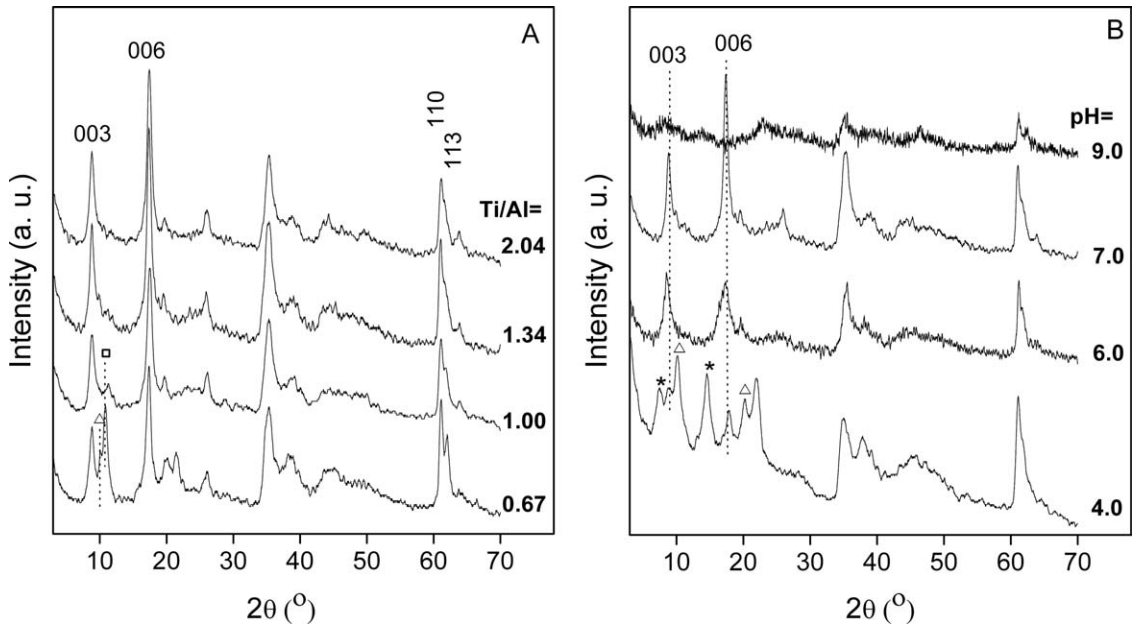


**Figure 4. XRD patterns of Ti-peroxide pillared Mg/Al LDH-coprecipitation prepared under different Ti/Al molar ratios (A) and pH values (B).**

Marked with □, Δ, and * are the coexisting Mg/Al—$CO_3$, Mg/Al—$NO_3$ and a second Ti-peroxide pillared LDH phase.

bonds, according to the previous assignment.[26] In the Raman spectra (Figure 5B), the bulk Ti-peroxide gel gives obvious bands at 895, 712, 668, 605, 493, and 289 $cm^{-1}$. The resonance at 668 $cm^{-1}$ and the remarkable one at 289 $cm^{-1}$ are assigned to the $\delta_{Ti—O}$ in Ti—O—Ti of solid Ti-peroxide according to the previous report.[37] Correspondingly, a broad band overlapping a few resonance bands arising from peroxo Ti—O—Ti linkages is observed at 493 $cm^{-1}$. Similar to FT-IR assignments, the Raman bands around 895 and 605 $cm^{-1}$ have been reported to arise from $\nu_s$ (O—O) and $\nu_s$ (Ti—$O_2$).[35,38] Intercalation of Ti-peroxide in the LDH interlayer region shifts $\nu_s$ (O—O) from 895 to 848 $cm^{-1}$. The intercalation also results in the absence of 668, 493, and 289 $cm^{-1}$, which are assigned to the Ti—O—Ti vibration. A new resonance at 684 $cm^{-1}$ emerges. The resonance at 684 $cm^{-1}$ could arise from either $\delta_{Ti—O}$ in Ti—O—Ti or $\delta_{C—O}$ in $CO_3^{2-}$. In the present case, the contribution from the $\delta_{C—O}$ of $CO_3^{2-}$ apparently dominates.

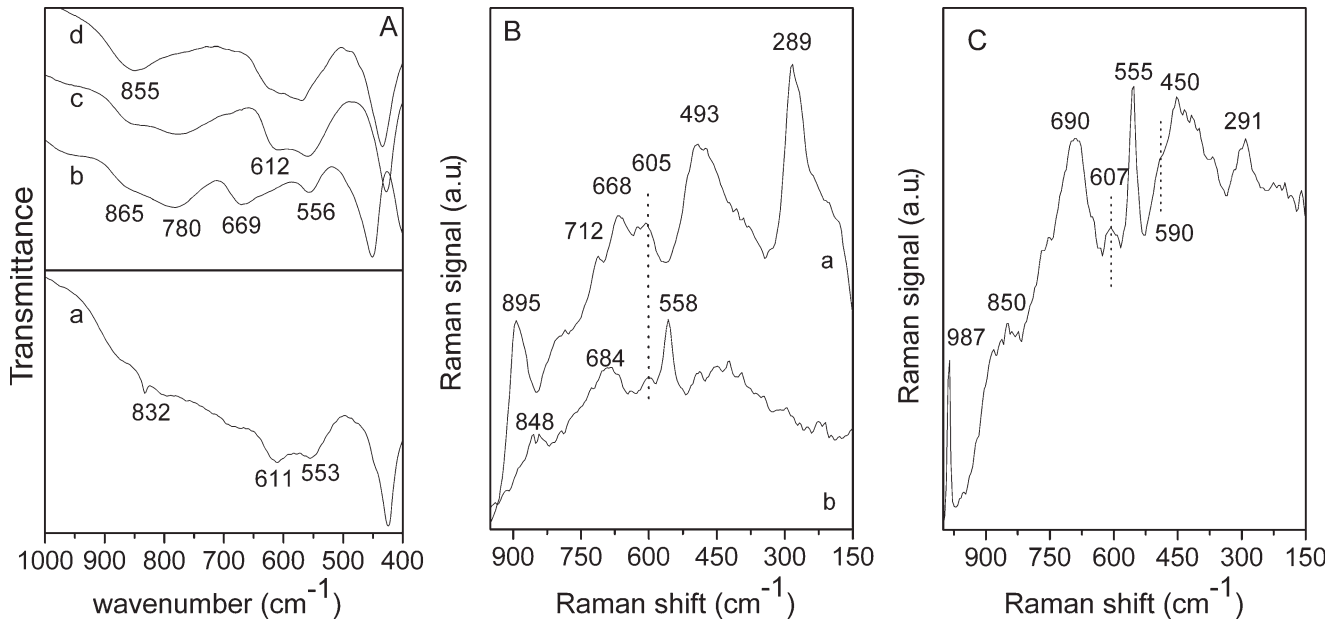


**Figure 5. FT-IR (A) and Raman (B) spectra of Ti-peroxide gel in bulk (a) and intercalated into Mg/Al LDH-coprecipitaion (b), Zn/Al LDH-coprecipitaion (c), and Ni/Al LDH-coprecipitaion (d); (C) Raman spectrum of thermally treated (b) at 60°C for 3 h.**

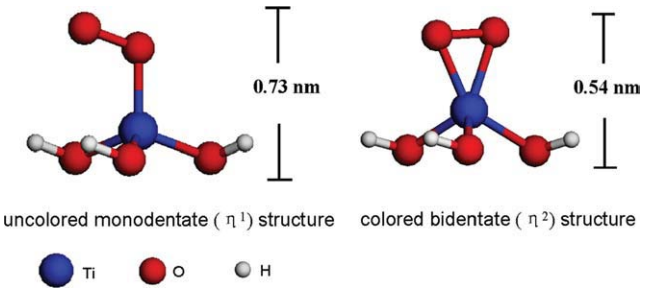


**Scheme 1. The schematic illustration of possible Ti-peroxide structures.**

[Color figure can be viewed in the online issue, which is available at www.interscience.wiley.com.]

The Ti-peroxide most popularly observed was bidentate ($\eta^2$) with $C_{2v}$ symmetry (Scheme 1).[39] The characteristic band of this triangular ($\eta^2$) structure of Ti—$O_2$ unit was proposed[38] to be around 890 or 610 $cm^{-1}$, both being resolved in this work. Additionally, in our experiments, the Ti-peroxide solution as intercalating precursor is found in yellowish color, characteristic of $\eta^2$-structured Ti-peroxide as well. So it is proposed that the Ti-peroxide anion is typically intercalated into the LDH interlayer regions in $\eta^2$-structure. The size of $\eta^2$-Ti—$O_2$ unit is estimated as ~0.54 nm, matching the interlayer gallery height of 0.50–0.60 nm observed by the XRD patterns in most cases. It was also found that, although the colored (yellowish) solution consisted mainly of $\eta^2$-structured Ti-peroxide, the interconversion of Ti-peroxo ($\eta^2$) to uncolored Ti-hydroperoxo ($\eta^1$) species (Scheme 1) might take place in aqueous medium.[39,40] The size of $\eta^1$-Ti—$O_2$ unit is estimated as ~0.73 nm, matching an interlayer gallery height of ~0.70–0.80 nm. The $\eta^1$-structured Ti-peroxide thus accounts for the second basal spacing ($d_{003}$ = 1.18 nm) observed in the XRD pattern when the intercalation is carried out at a pH of 4.0.

Figure 6 illustrates the in situ temperature-programmed XRD patterns, as well as the change of basal spacing with temperature, of Ti-peroxide pillared Mg/Al LDH-coprecipitation. The pillared layered structures are well retained till 100°C and collapse at 400°C. The XRD peaks start to deform from 200°C, although the pillared structure can be considered as still present. The basal spacing decreases with increasing temperature. The decrease is relatively sharp below 100°C, especially from 40 to 60°C. This means some variation might occur to the interlayer anions in the thermal treatment. TG-MS analysis was thus performed. The TG curve for Ti-peroxide pillared Mg/Al LDH-coprecipitation consists of two weight losses at 30–220 and 230–370°C. The tracking mass spectra (summarized in Table 2) indicate that the segments released at 30°C are —OH and $H_2O$, and $O_2$ and $(OH)_2$ at 60°C. The —OH and $H_2O$ are additionally released at higher temperature regions. $CO_2$ emits principally above 310°C, which unequivocally result from the decomposition of interlayer $CO_3^{2-}$ coexisting with Ti-peroxide. The trace amount of $CO_2$ at 30–103°C originates from what was adsorbed physically. The —OH and $H_2O$ detected above 250°C arise from the dehydroxylation of LDH layers. Emitted in the range of 145–230°C are the interlayer $H_2O$ molecules. The —OH below 150°C, $H_2O$ below 105°C, and $(OH)_2$ below 130°C are supposed to result from the intramolecular or intermolecular dehydroxylation of interlayer Ti-peroxide species. The breakage of —O—O— bonds accounts for the $O_2$ release at 60–145°C. The Raman spectrum of Ti-peroxide pillared Mg/Al LDH-coprecipitation after thermal treatment at 60°C for 3 h confirms the changes speculated earlier. In the Raman spectrum (Figure 5C), obvious Raman resonances at 291 and 450 $cm^{-1}$ originating from Ti—O—Ti and characteristic of Ti=O at 987 $cm^{-1}$ are observed, in addition to the Raman bands at 555 $cm^{-1}$ characteristic of LDH layer M—OH, 607 $cm^{-1}$ assigned to $\nu_s$ (Ti—$O_2$), 690 $cm^{-1}$ arising from Ti—O—Ti, and 850 $cm^{-1}$ representing $\nu_s$ (O—O). The Ti—O—Ti linkages, which have been prevented from formation by intercalation, are formed in the thermal

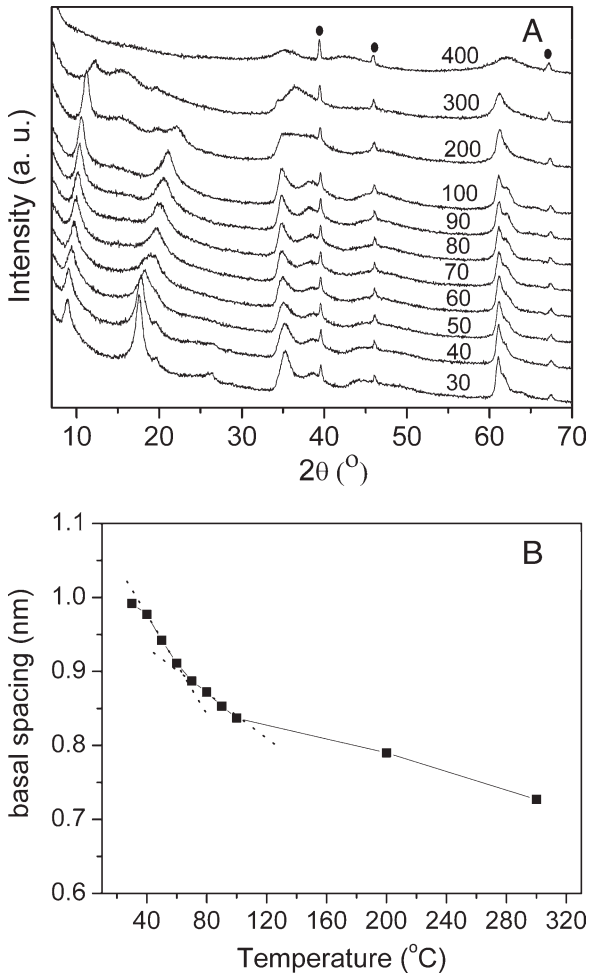


**Figure 6. Temperature-programmed XRD patterns of Ti-peroxide pillared Mg/Al LDH-coprecipitaion (A) and the basal spacing vs. temperature (B).**

**Table 2. The TG-MS Segments of Ti-Peroxide Pillared Mg/Al LDH-Coprecipitation**

| *m/z* | Segment | Region (I) (°C) | Region (II) (°C) | Region (III) (°C) |
|---|---|---|---|---|
| 32 | $O_2$ | 60–145 | | |
| 34 | $-(OH)_2$ | 60–130 | | |
| 17 | —OH | 30–130 | 130–150 | 250–360 |
| 18 | $H_2O$ | 30–105 | 145–230 | 270–350 |
| 44 | $CO_2$ | 30–105 | | 275–345 |

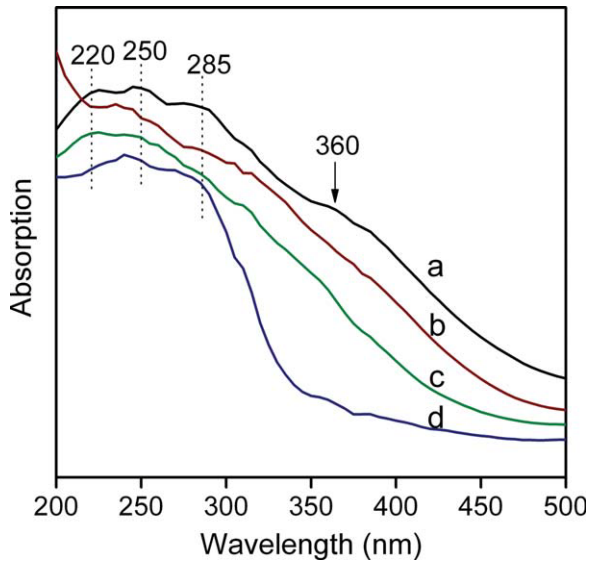


**Figure 7. UV–vis diffuse reflectance spectra of Ti-peroxide (a) gel in bulk, (b) intercalated into the interlayer of Mg/Al LDH-coprecipitaion, (c) thermally treated at 60°C for 1 h, and (d) thermally treated (b) at 200°C for 1 h.**

[Color figure can be viewed in the online issue, which is available at www.interscience.wiley.com.]

treatment because of the intermolecular dehydroxylation of interlayer Ti-peroxide species. The interamolecular dehydroxylation results in the formation of Ti=O linkage. On account of the thermal stability of interlayer Ti-peroxide, a reaction temperature of up to 60°C is applicable to the intercalated Ti-peroxide, which is a typical temperature range most commonly used for the liquid-phase oxidations.

The UV–vis diffuse reflectance spectra shown in Figure 7 confirm the earlier results from Raman spectra and TG-MS analysis. As can be seen in Figure 7, the Ti-peroxide gel in bulk exhibits resolved absorption at 220, 250, and 285 nm. A weak shoulder around 360 nm is also observed. According to the previous study,[41] the absorption around 200–250 nm results from isolated tetrahedral Ti(IV), and the absorption at 250 and 285 nm is associated with isolated Ti(IV) in five- and sixfold coordination. The absorption above 350 nm originates from $TiO_2$. For the Ti-peroxide intercalated into LDHs, only one dominating absorption at 240 nm is observed, hinting that the interlayer Ti(IV) is located in relatively uniform coordination. The mild thermal treatment (at 60°C) causes no marked changes in the UV–vis absorption. After treatment at 200°C, the absorption at 285 nm becomes visible. But no absorption above 300 nm can be resolved. This result further indicates that the intercalation prevents the polymerization of Ti-peroxides and also enhances the thermal stability.

### *Catalytic properties*

The Ti-peroxides intercalated into the LDH interlayer regions are used as catalyst for the oxidation of phenyl methyl sulfide using aqueous $H_2O_2$ as oxidant. The conversion and selectivity on each catalyst are shown in Table 3. Because the combination of HOOH and acetonitrile is the so-called Payne-Reagent, which might have oxidizing properties by itself, several blank experiments have been performed (Table 3). As can be seen in Table 3, the catalytic oxidation of phenyl methyl sulfide takes place readily on all the Ti-peroxide pillared LDHs prepared in this work. In comparison to the conversions in blank reactions with or without LDHs introduced, the LDH solids with Ti-peroxide intercalated display much higher oxidizing activity. It means that the thioether conversion mainly originates from the catalytic property of Ti-peroxide centers. The oxidation products consist of sulfoxide and sulfone. But in each case, more sulfoxide is yielded than sulfone, and no other products have been detected.

**Table 3. The Selective Oxidation of Phenzyl Methyl Sulfide Catalyzed by Ti-Peroxide Pillared LDHs***

| | Conversion (%) | TON | Selectivity (%) | |
|---|---|---|---|---|
| | | | Sulfoxide | Sulfone |
| $H_2O_2$ | 11 | – | 75 | 25 |
| Pristine Mg/Al-coprecipitation | 4 | – | 96 | 4 |
| Pristine Zn/Al-coprecipitation | 16 | – | 81 | 19 |
| Pristine Ni/Al-coprecipitation | 6 | – | 93 | 7 |
| Ti-peroxide pillared Mg/Al-coprecipitation | 51 | 12 | 67 | 33 |
| Ti-peroxide pillared Mg/Al-homogeneous | 41 | 18 | 56 | 44 |
| Ti-peroxide pillared Zn/Al-coprecipitation | 38 | 15 | 74 | 26 |
| Ti-peroxide pillared Ni/Al-coprecipitation | 32 | 21 | 68 | 32 |

*Reaction time = 11 h.

It can also be found from Table 3 that the TON on Ti-peroxide pillared Ni/Al LDH is higher than on Ti-peroxide pillared Mg/Al and Zn/Al LDHs. More interesting, even though the Mg/Al LDH-homogeneous and Mg/Al LDH-coprecipitation are composed of resembling host layers, the Ti-peroxide in the interlayer regions of Mg/Al LDH-homogeneous turns out a better oxidizing ability (higher TON and lower selectivity to sulfoxide) than that in Mg/Al LDH-coprecipitation. This observation is reasonable when taking into consideration the role of hydrogen bond between the interlayer Ti-peroxide and LDH host layers. As well recognized,[42] the layer structure of LDHs is based on that of brucite $[Mg(OH)_2]$ with a fraction of divalent cations substituted by trivalent cations. It consists of metal ions surrounded approximately octahedrally by hydroxide ions. These octahedral units form infinite layers in 0.21 nm thickness by edge sharing, with the

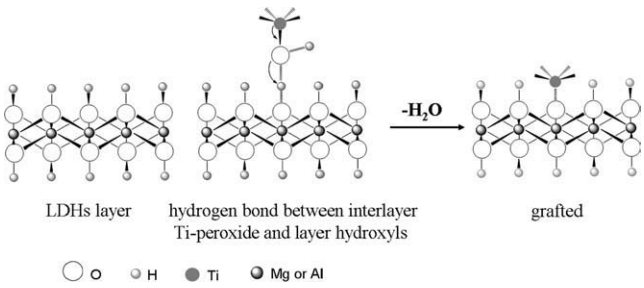


**Scheme 2. The schematic illustration of LDH layers and interactions between interlayer Ti-peroxide and LDH layers.**

hydroxide ions sitting perpendicular to the plane of the layers, as shown in Scheme 2. The layer hydroxyl groups in LDHs can act as hydrogen bond donors to both the interlayer Ti-peroxide and the oxygen atoms of interlayer water molecules. The interlayer water molecules, which may also form hydrogen bonds between themselves, can also act as hydrogen bond donors to the interlayer Ti-peroxide. The thickness of the hydrogen bonding region in between two LDH layers sums up to ~0.27 nm. The hydrogen bonds between the interlayer Ti-peroxide and layer hydroxyl groups/interlayer water molecules consequently reduce the electron density of Ti—O—O sites (Scheme 2). Reduced electron density means increased electrophilicity, facilitating the nucleophilic attack of S atom in thioether. Highly crystallized LDHs possess much better-ordered lattice structure and more regularly arranged layer hydroxyls[43] than poorly crystallized LDHs, promoting the hydrogen bonding of Ti-peroxide to the host layers. As has been resolved earlier, Mg/Al LDH-homogeneous is much better crystallized than Mg/Al LDH-coprecipitation, accounting for the higher activity of Ti-peroxide pillared Mg/Al LDH-homogeneous. As for Ti-peroxide pillared Ni/Al LDH, the Ni(II) with vacant 3d orbits in the LDH host layers could accelerate the hydrogen bonding, responsible for the higher TON.

### *Recyclability*

Ti-peroxide intercalated Mg/Al LDH-coprecipitation is recovered by simple filtration or centrifugation and recycled for the catalytic oxidation of phenyl methyl sulfide. The variations of thioether conversion and sulfoxide selectivity with run number are shown in Figure 8. For comparison, the results for Ti-peroxides in bulk and adsorbed on the Mg/Al—$CO_3$ LDH surface are also illustrated. For the Ti-peroxide in bulk, the oxidation ability stay stable in the first two runs but decreases apparently thereafter. A quite low conversion and higher sulfoxide selectivity is observed in the fourth run. The oxidation ability of the Ti-peroxide adsorbed on the exterior surface of Mg/Al—$CO_3$ LDH particles is reduced gradually in the recycle in that the observed conversion decreases and the sulfoxide selectivity increases with recycle number. The oxidation ability of Ti-peroxide encapsulated in the interlayer regions of LDH-coprecipitation decreases in the first recycle run but then stays steady. So it is reasonable to deduce that the encapsulation of Ti-peroxide in the LDH interlayers inhibits the loss of catalytic activity. The positively charged layers preserve and disperse the interlayer Ti-peroxide anions through electrostatic attraction, which is not present for Ti-peroxide either in bulk or adsorbed on the exterior surface of LDH particles. The virtue of recyclability for Ti-peroxide pillared Mg/Al LDH-coprecipitation is reasonably explained by the structural stability. The XRD pattern for the recycled Ti-peroxide pillared LDHs, shown in Figure 9A, indicates that in the sulfoxidation no obvious change occurs to the pillared layered structure. The Mg/Al and Ti/Al molar ratios in the recycled Ti-peroxide pillared LDHs, determined by ICP technique, are 2.05 and 0.60, showing no difference from the fresh catalyst (2.05 and 0.61, respectively). No leached Ti has been detected in the final reaction supernatant as well.

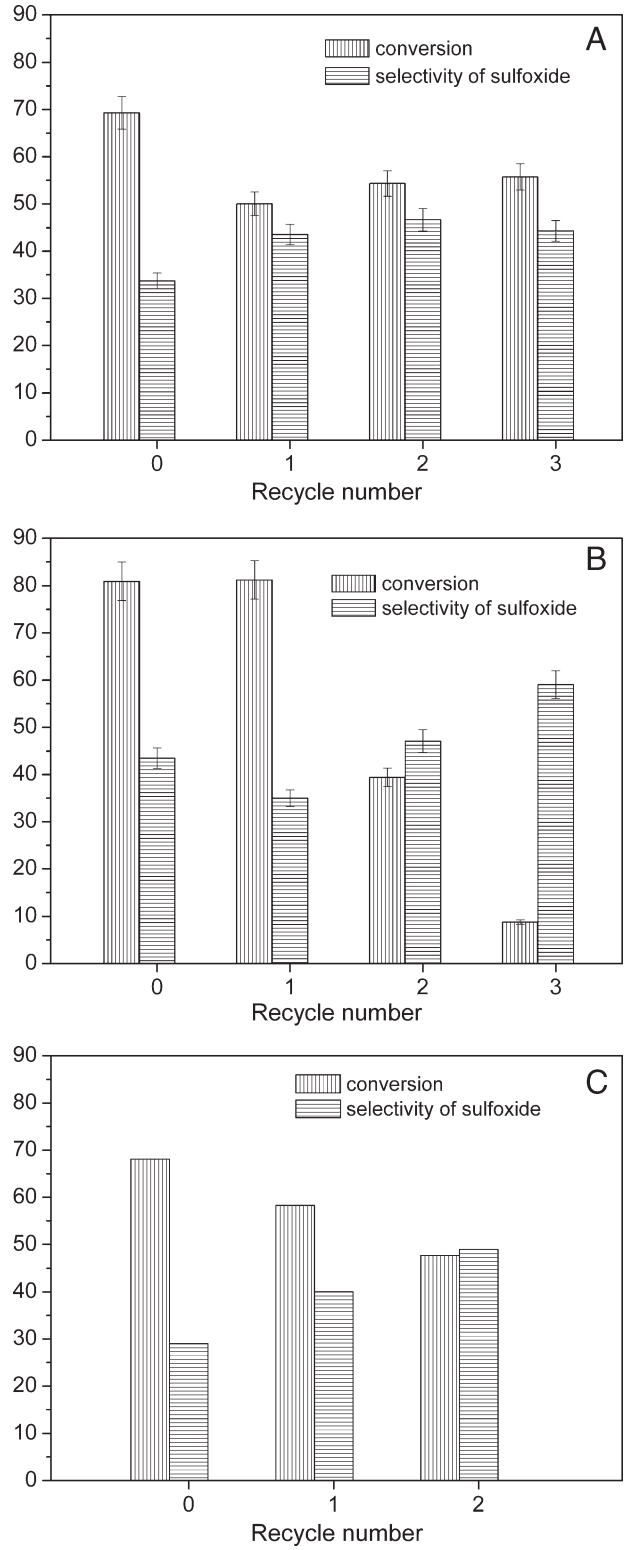


**Figure 8. Recycle of Ti-peroxide (A) intercalated into the interlayer of Mg/Al LDH-coprecipitaion, (B) gel in bulk, and (C) adsorbed on the exterior surface of Mg/Al—$CO_3$ LDH-coprecipitaion.**

However, the Ti-peroxide pillared Mg/Al LDH-homogeneous behaves dissimilarly to Ti-peroxide pillared Mg/Al LDH-coprecipitation in the recycle. As shown in Figure 10, the conversion of phenyl methyl sulfide on Ti-peroxide pillared Mg/Al LDH-homogeneous gradually decreases with recycle number. Similar to Ti-peroxide pillared Mg/Al LDH-coprecipitation, ICP analysis indicates no obvious Ti leaching. But the XRD pattern (Figure 9B) of Ti-peroxide pillared Mg/Al LDH-homogeneous changes in the catalytic recycle. As illustrated in Figure 9B, additional (003) and (006) reflections with a basal spacing of 0.89 nm are observed for the recycled catalyst besides what is observed at 1.18 nm for the fresh one. The basal spacing for the newly emerged intercalation phase is similar to that for nitrate-pillared LDHs. But no N element can be detected in both fresh and used Ti-peroxide pillared Mg/Al LDH-homogeneous. So the second (003) and (006) reflections should also originate from the Ti-peroxide pillared LDHs. The new basal spacing is 0.29 nm smaller than 1.18 nm, which corresponds to the thickness (0.27 nm) of interlayer hydrogen bonding region. So it is most possible that grafting reaction between the layer hydroxyl and Ti—O—H has occurred (Scheme 2). In the catalytic reaction, the nucleophilic attack of thioether molecules could inversely accelerate the hydrogen bond between interlayer Ti-peroxide and LDH layer hydroxyls, and even promote the grafting, especially in the case of highly crystallized LDHs as host. The occurrence of —Ti—O— grafting to LDH layers causes the appearance of the new pillared phase in the used catalyst (Figure 9B). In comparison to —Ti—O—H, the grafted —Ti—O— linkage is difficult or impossible to get activated with $H_2O_2$, which explains the activity loss in the recycle of Ti-peroxide pillared Mg/Al LDH-homogeneous. Relatively, Mg/Al LDH-coprecipitation is less crystallized and has more layer hydroxyl deficiencies, partially contributing to the good recyclability of Mg/Al LDH- coprecipitation as catalyst.

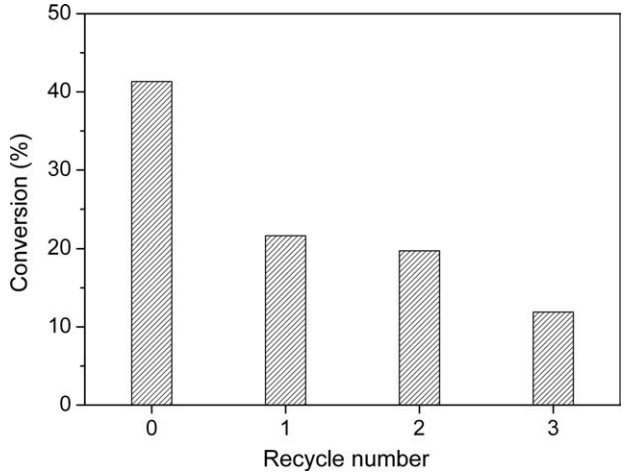


**Figure 10. Recycle of Ti-peroxide intercalated into the interlayer of Mg/Al LDH-homogeneous.**

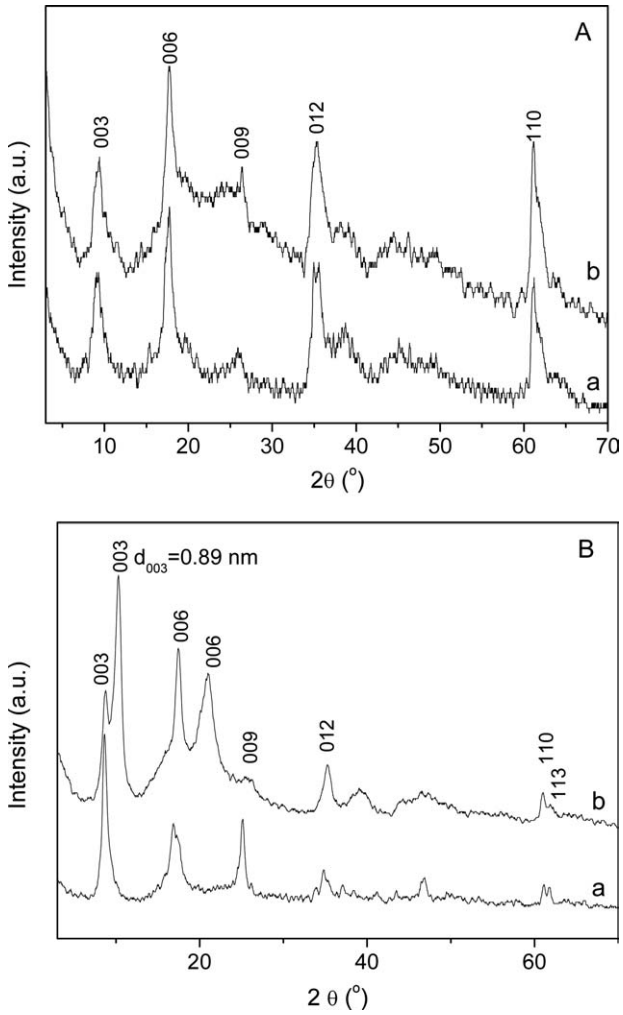


**Figure 9. XRD patterns of Ti-peroxide pillared Mg/Al LDH-coprecipitation (A) and Mg/Al LDH-homogeneous (B).**

(a) Before and (b) after catalytic sulfoxidation.

No obvious evidence could be clearly presented in this work to support whether the sulfoxidation took place in the center or at the edge of interlayer regions or even just on the exterior surface of LDH particles. Yet the recyclability of Ti-peroxide pillared Mg/Al LDH-coprecipitation and the structural alteration of Ti-peroxide pillared Mg/Al LDH-homogeneous in the recycle use at least hint the indispensable catalytic role of interlayer Ti species.

## Conclusions

In summary, Ti(IV)-peroxide pillared layered metal hydroxides have been prepared in this work for the first time through the intercalation of environmental-benign, water-soluble Ti-peroxide precursor. The preparation procedures involve no usage of organic or chlorine-containing hazards. The resulting Ti-pillared layered solids show a great potential as catalyst for the selective oxidation of sulfide compounds. The chemical composition and crystallinity of LDH host layers work on the catalytic performance of Ti-peroxide pillared LDHs in the sulfoxidation by virtue of the hydrogen bonding of host layer hydroxyls to interlayer Ti-peroxide. The Ti-peroxide pillared Mg/Al LDHs with particle sizes of around 50–120 nm exhibits good stability and recyclability.

## Acknowledgments

The authors are grateful to the financial support from NSFC and "973" Program (2009CB939802).

## Literature Cited

1. Arends IWCE, Sheldon RA. Activities and stabilities of heterogeneous catalysts in selective liquid phase oxidations: recent developments. *Appl Catal A*. 2001;212:175–187.
2. Alaerts L, Wahlen J, Jacobs PA, De Vos DE. Recent progress in the immobilization of catalysts for selective oxidation in the liquid phase. *Chem Commun*. 2008;1727–1737.
3. Kholdeeva OA, Trukhan NN. Mesoporous titanium silicates as catalysts for the liquid-phase selective oxidation of organic compounds. *Russ Chem Rev*. 2006;75:411–432.
4. Taramasso M, Perego G, Notari B. US Patent4 410 501 to Enichem.
5. Gündüz G, Dimitrova R, Yilmaz S, Dimitrov L. Liquid phase transformation of α-pinene over beta zeolites containing aluminium or boron, titanium and vanadium as lattice ions. *Appl Catal A*. 2005;282:61–65.
6. Camblor MA, Corma A, Esteve P, Martínez A, Valencia S. Epoxidation of unsaturated fatty esters over large-pore Ti-containing molecular sieves as catalysts: important role of the hydrophobic–hydrophilic properties of the molecular sieve. *Chem Commun*. 1997;795–796.
7. Araújo RS, Azevedo DCS, Rodríguez-Castellón E, Jiménez-López A, Cavalcante CL Jr. Al and Ti-containing mesoporous molecular sieves: synthesis, characterization, and redox activity in the anthracene oxidation. *J Mol Catal A*. 2008;281:154–163.
8. Cimpeanu V, Pârvulescu AN, Pârvulescu VI, On DT, Kaliaguine S, Thompso JM, Hardacre C. Liquid-phase oxidation of a pyrimidine thioether on Ti-SBA-15 and UL-TS-1 catalysts in ionic liquids. *J Catal*. 2005;232:60–67.
9. Chandra D, Laha SC, Bhaumik A. Highly porous organic–inorganic hybrid silica and its titanium silicate analogs as efficient liquid-phase oxidation catalysts. *Appl Catal A*. 2008;342:29–34.
10. He J, Wei M, Li B, Kang Y, Evans DG, Duan X. Preparation of layered double hydroxides. *Struct Bond*. 2006;119:89–119.
11. Cavani F, Trifirò F, Vaccari A. Hydrotalcite-type anionic clays: preparation, properties and applications. *Catal Today*. 1991;11:173–301.
12. Centi G, Perathoner S. Catalysis by layered materials: a review. *Micropor Mesopor Mater*. 2008;107:3–15.
13. Li F, Duan X. Application of layered double hydroxides. *Struct Bond*. 2005;119:193–223.
14. Zhang GK, Ding XM, He FS, Yu XY, Zhou J, Hu YJ, Xie JW. Low-temperature synthesis and photocatalytic activity of $TiO_2$ pillared montmorillonite. *Langmuir*. 2008;24:1026–1030.
15. Motokura K, Fujita N, Mori K, Mizugaki T, Ebitani K, Kaneda K. An acidic layered clay is combined with a basic layered clay for one-pot sequential reactions. *J Am Chem Soc*. 2005;127:9674–9675.
16. Ebitani K, Kawabata T, Nagashima K, Mizugaki T, Kaneda K. Simple and clean synthesis of 9,9-bis[4-(2-hydroxyethoxy)phenyl]fluorene from the aromatic alkylation of phenoxyethanol with fluoren-9-one catalysed by titanium cation-exchanged montmorillonite. *Green Chem*. 2000;2:157–160.
17. Yuan P, Yin X, He H, Yang D, Wang L, Zhu J. Investigation on the delaminated-pillared structure of $TiO_2$-PILC synthesized by $TiCl_4$ hydrolysis method. *Micropor Mesopor Mater*. 2006;93:240–247.
18. Sterte J. Synthesis and properties of titanium oxide cross-linked montmorillonite. *Clay Clay Miner*. 1986;34:658–664.
19. Yamanaka S, Nishihara T, Hattori M, Suzuki Y. Preparation and properties of titania pillared clay. *Mater Chem Phys*. 1987;17:87–101.
20. Bineesh KV, Cho DR, Kim SY, Jermy BR, Park DW. Vanadia-doped titania-pillared montmorillonite clay for the selective catalytic oxidation of $H_2S$. *Catal Commun*. 2008;9:2040–2043.
21. Gardner E, Pinnavaia TJ. On the nature of selective olefin oxidation catalysts derived from molybdate and tungstate-intercalated layered double hydroxides. *Appl Catal A*. 1998;167:65–74.
22. Pillai UR, Sahle-Demessie E. Sn-exchanged hydrotalcites as catalysts for clean and selective Baeyer-Villiger oxidation of ketones using hydrogen peroxide. *J Mol Catal A*. 2003;191:93–100.
23. Villa AL, De Vos DE, Verpoort F, Sels BF, Jacobs PA. A study of V-pillared layered double hydroxides as catalysts for the epoxidation of terpenic unsaturated alcohols. *J Catal*. 2001;198:223–231.
24. Zavoianu R, Bîrjega R, Pavel OD, Cruceanu A, Alifanti M. Hydrotalcite like compounds with low Mo-loading active catalysts for selective oxidation of cyclohexene with hydrogen peroxide. *Appl Catal A*. 2005;286:211–220.
25. Kakihana M, Tomita K, Petrykin V, Tada M, Sasaki S, Nakamura Y. Chelating of titanium by lactic acid in the water-soluble diammonium tris(2-hydroxypropionato) titanate(IV). *Inorg Chem*. 2004;43:4546–4548.
26. Tomita K, Petrykin V, Kobayashi M, Shiro M, Yoshimura M, Kakihana M. A water-soluble titanium complex for the selective synthesis of nanocrystalline brookite, rutile, and anatase by a hydrothermal method. *Angew Chem Int Ed Engl*. 2006;45:2378–2381.
27. Camargo ER, Frantti J, Kakihana M. Low-temperature chemical synthesis of lead zirconate titanate (PZT) powders free from halides and organics. *J Mater Chem*. 2001;11:1875–1879.
28. Ayers MR, Hunt AJ. Titanium oxide aerogels prepared from metal titanium and hydrogen peroxide. *Mater Lett*. 1998;34:290–293.
29. Padmanabhan S, Lavin RC, Durant GJ. Asymmetric synthesis of a neuroprotective and orally active *N*-methyl-D-aspartate receptor ion-channel blocker, CNS 5788. *Tetrahedron: Asymmetry*. 2000;11:3455–3457.
30. Madhusudhan RG, Kaga M, Vijaya BB, Pratap RP. Synthesis of metabolites and related substances of rabeprazole, an anti-ulcerative drug. *Synth Commun*. 2009;39:278–290.
31. Li L, Ma R, Ebina Y, Iyi N, Sasaki T. Positively charged nanosheets derived via total delamination of layered double hydroxides. *Chem Mater*. 2005;17:4386–4391.
32. Prévot V, Forano C, Besse JP. Intercalation of anionic oxalato complexes into layered double hydroxides. *J Solid State Chem*. 2000;153:301–309.
33. Beaudot P, de Roy ME, Besse JP. Intercalation of platinum complex in LDH compounds. *J Solid State Chem*. 2001;161:332–340.
34. Muhlebach J, Muller K, Schwarzenbach G. The peroxo complexes of titanium. *Inorg Chem*. 1970;9:2381–2390.
35. Dakanali M, Kefalas ET, Raptopoulou CP, Terzis A, Voyiatzis G, Kyrikou I, Mavromoustakos T, Salifoglou A. A new dinuclear Ti(IV)-peroxo-citrate complex from aqueous solutions. Synthetic, structural, and spectroscopic studies in relevance to aqueous titanium(IV)-peroxo-citrate speciation. *Inorg Chem*. 2003;42:4632–4639.
36. Kholdeeva OA, Trubitsina TA, Maksimovskaya RI, Golovin AV, Neiwert WA, Kolesov BA, López X, Poblet JM. First isolated active titanium peroxo complex: characterization and theoretical study. *Inorg Chem*. 2004;43:2284–2292.
37. Tengvall P, Vikinge TP, Lundstrom I, Liedberg B. FT-Raman spectroscopic studies of the degradation of titanium peroxy gels made from metallic titanium and hydrogen peroxide. *J Colloid Interface Sci*. 1993;160:10–15.
38. Nour EM, Morsy S. Resonance Raman studies of the peroxotitanate(IV) complexes $K_2(Ti(O_2)(SO_4)_2)\cdot 5H_2O$ and $K_2(Ti(O_2)C_2O_4)_2)\cdot 3H_2O$. *Inorg Chim Acta*. 1986;117:45–48.
39. Bonino F, Damin A, Ricchiardi G. Ti-peroxo species in the TS-1/$H_2O_2$/$H_2O$ system. *J Phys Chem B*. 2004;108:3573–3583.
40. Spanó E, Tabacchi G, Gamba A, Fois E. On the role of Ti(IV) as a Lewis acid in the chemistry of titanium zeolites: formation, structure, reactivity, and aging of Ti-peroxo oxidizing intermediates. A first principles study. *J Phys Chem B*. 2006;110:21651–21661.
41. Klein S, Weckhuysen BM, Martens JA, Maier WF, Jacobs PA. Homogeneity of titania-silica mixed oxides: on UV-DRS studies as a function of titania content. *J Catal*. 1996;163:489–491.
42. Evans DG, Slade RCT. Structural aspects of layered double hydroxides. *Struct Bond*. 2006;119:1–87.
43. Lei X, Zhang F, Yang L, Guo X, Tian Y, Fu S, Li F, Evans DG, Duan X. Highly crystalline activated layered double hydroxides as solid acid–base catalysts. *AIChE J*. 2007;53:932–940.

*Manuscript received Mar. 30, 2009, and revision received July 3, 2009.*